

Increasing the Image Sharpness with Linear Operator for Social Internet-Services

Prystavka Pylyp ¹ [0000-0002-0360-2459], Cholyshkina Olha ² [0000-0002-0681-0413]
and Zhengbing Hu ² [0000-0002-6140-3351]

¹National Aviation University, Komarova 1, Kyiv, Ukraine

²Interregional Academy of Personal Management, Frometivska 2, Kyiv, Ukraine

³Central China Normal University, Wuhan, China

greenhelga5@gmail.com

Abstract. In the paper it has been propounded and experimentally researched the linear operators that can be used to sharpen digital images or video frames distorted by a micro-motion of fixation chamber. It has been assumed that the cause of the problem, which leads to deterioration of sharpness, is a low-frequency interference, which is exemplified by a random non-recursive filter in the form of a discrete convolution. It has been experimentally proven that the proposed stabilizer filters allow for significant visual enhancement of distorted images, with a peak-to-peak signal-to-noise ratio for the improved images higher than if using similar sharpening filters implemented in Adobe PhotoShop CS6. The corresponding masks of the proposed operators and the examples of application are given in the paper.

Keywords: Image processing, image sharpness, digital stabilization, *B*-spline, linear filter operators.

1. Topicality and problem statement

An important factor for the positive perception of a digital image, or video stream, as a sequence of frames is how realistic it is. At the same time the sharpness of an image is one of the constituents that determine the realness of the image. The main causes for distortion that lead to deterioration of clarity are the limited resolution capabilities of the forming system, defocus, the presence of the distorting medium (such as the atmosphere), the movement of the camera towards the object which is being recorded [1]. Further we shall consider the processing of images obtained under the conditions of the micro-motion of the fixation chamber. This defect is most common in the case of a photography without a tripod or if shooting from a platform that may be a subject to some mechanical impact, such as microvibration (aerophotography, etc.). Unlike other cases, the consequences of micro-motion can be eliminated or at least significantly offset, not only by hardware but also by mathematical treatment procedures. Therefore, we believe the topical task is to find appropriate procedures for image sharpening. These should have low computational complexity and upon implementa-

Copyright © 2020 for this paper by its authors. Use permitted under Creative Commons License Attribution 4.0 International (CC BY 4.0) CMiGIN-2019: International Workshop on Conflict Management in Global Information Networks.

tion in software products they should provide real-time processing.

In assumption of isoplanatic system of observation for intensity distribution $I(x)$ the image of the object, that is being formed in the x plane of its registration, is being used an expression of the following type [2]:

$$I(x) = \int O(y)H(x-y)dy, \quad (1)$$

where $O(y)$ - the distribution of the intensity of reflection from the object of light irradiation in the image plane y ; $H(x)$ - distribution of intensity in the image of an axial source point (impulse response or else – scattering of the function system point). Expression (1) provides an image that is recorded in the form of a convolution of a true image and the impulse response of the registration system. Thus [1], the intensity value of the original image is "smeared" at each of the points of registration in accordance with the type of function $H(x)$.

To fix the problems caused by the micro-movement of the fixation chamber, they use image stabilizers, which can be divided into three general types [3; 4]: mechanical, electronic and digital. In this paper we research namely digital stabilizers. They are not used to against the cause of the blurry images in photo and video material. On the contrary they are intended to eliminate the consequences - that is, they are used for the post-fixation mathematical processing of digital data.

There is a number of methods used to reproduce blurred images [1; 2; 5; 7-9]. However, among the effective procedures of digital image sharpening (digital stabilization) that satisfy the requirements of actual processing in real time, preference should be given to those that achieve the target processing function at a minimum of computational operations. In fact, these are linear operators obtained in the form of a discrete convolution of the color components of the raster and masks of filters-stabilizers.

Assuming that the distortion of the original image has been caused by the micro-motion of the locking chamber, as e.g. by the vibration of the aircraft during aerial photography [6], then, according to the above-mentioned and based on (1), the following representation can be considered reasonable for a digital image

$$p_{i,j} = L(p^{i,j}) = \sum_{ii=i-r_i}^{i+r_i} \sum_{jj=j-r_j}^{j+r_j} \gamma_{ii-i, jj-j} p_{ii, jj}^0, \quad i = \overline{-\frac{k_i}{2}, \frac{k_i}{2}}, \quad j = \overline{-\frac{k_j}{2}, \frac{k_j}{2}}, \quad (2)$$

where $p_{i,j}$ - color raster component (red, green or blue); $L(i,j)$ - linear low-pass image filter operator; (i,j) - the pixel index of the raster; k_i, k_j - image frame sizes; $p_{ii, jj}^0$ - the color component of the raster of the perfect undistorted image; $\gamma_{ii-i, jj-j}$ - low pass filter mask element; $(2r_i + 1) \times (2r_j + 1)$ - the size of the low pass filter mask.

Considering a digital image, specified by the raster with any of the constituents $P = \{p_{i,j}; i = \overline{0, H-1}, j = \overline{0, W-1}\}$. As an experiment, we will simulate an accidental low-frequency interference, such as the operator (2), for some digital images. To obtain a linear operator $L(p^{ij})$ from (2), we shall define the low pass filter mask as follows.

Assumingly $\{p_i^\circ\}_{i \in \mathbb{Z}}$ - one-dimensional sequence of a function (for distinctness), and $\{p_i\}_{i \in \mathbb{Z}}$ - a sequence obtained after smoothing. If

$$p_i = p_i^\circ + \alpha \Delta^2 p_i^\circ + \beta \Delta^4 p_i^\circ,$$

where

$$\begin{aligned} \Delta^2 p_i^\circ &= p_{i-1}^\circ - 2p_i^\circ + p_{i+1}^\circ; \\ \Delta^4 p_i^\circ &= \Delta^2 p_{i-1}^\circ - 2\Delta^2 p_i^\circ + \Delta^2 p_{i+1}^\circ, \end{aligned} \quad (3)$$

$$\alpha \in [0, 0,5; 0,5],$$

then

$$p_i = \beta p_{i-2}^\circ + (\alpha - 4\beta) p_{i-1}^\circ + (1 - 2\alpha + 6\beta) p_i^\circ + (\alpha - 4\beta) p_{i+1}^\circ + \beta p_{i+2}^\circ,$$

hence, from the condition of additionality (as for the low pass filter) with the coefficients p_i° , $i \in \mathbb{Z}$, we get:

$$\begin{cases} \beta \geq 0, \\ \alpha - 4\beta \geq 0, \\ 1 - 2\alpha + 6\beta \geq 0, \end{cases} \quad \begin{cases} \beta \geq 0, \\ \beta \leq 0, 25\alpha, \\ \beta \geq 0, 333 \cdot (\alpha - 0,5), \end{cases} \quad \beta \in [0; 0, 25\alpha]. \quad (4)$$

With the direct multiplication it is not difficult to obtain a low-pass filter mask of size 5x5 to determine the operator (2), namely (taking into account the symmetry):

$$\gamma = \begin{pmatrix} \beta^2 & \alpha\beta - 4\beta^2 & \beta - 2\alpha\beta + 6\beta^2 & \dots \\ \alpha\beta - 4\beta^2 & (\alpha - 4\beta)^2 & (\alpha - 4\beta)(1 - 2\alpha + 6\beta) & \dots \\ \beta - 2\alpha\beta + 6\beta^2 & (\alpha - 4\beta)(1 - 2\alpha + 6\beta) & (1 - 2\alpha + 6\beta)^2 & \dots \\ \vdots & \vdots & \vdots & \ddots \end{pmatrix},$$

where α and β are defined as evenly distributed random realizations that satisfy conditions (3) and (4).

Linear operator for the digital stabilization of images

Let's introduce linear operators $C(p^y)$ of digital image's stabilization, as follows

$p_{i,j}^* = C(p^{ij})$, and the quality of stabilization will be considered acceptable if considering (2) true is

$$p_{i,j}^* \approx p_{i,j}^o, \quad i, j \in \mathbb{Z} \quad (5)$$

for a random mask γ .

Linear operators, such as those considered in [6], can be used to stabilize the image:

$$C_l(p^{ij}) = \sum_{ii=i-\eta}^{i+\eta} \sum_{jj=j-\eta}^{j+\eta} \gamma_{ii-i, jj-j}^{(l)} p_{ii, jj}, \quad i, j \in \mathbb{Z}, \quad (6)$$

Where $l=0,1,2,3,4; r_0=2; r_1=r_2=3; r_3=r_4=4;$

$$\gamma^{(0)} = \frac{1}{3136} \begin{pmatrix} 1 & 8 & -74 & 8 & 1 \\ 8 & 64 & -592 & 64 & 8 \\ -74 & -592 & 5476 & -592 & -74 \\ 8 & 64 & -592 & 64 & 8 \\ 1 & 8 & -74 & 8 & 1 \end{pmatrix};$$

$$\gamma^{(1)} = \begin{pmatrix} 3,75457E-09 & 8,93587E-07 & 5,40282E-06 & -7,38748E-05 & \dots \\ 8,93587E-07 & 0,000212674 & 0,001285871 & -0,01758221 & \dots \\ 5,40282E-06 & 0,001285871 & 0,007774658 & -0,106305883 & \dots \\ -7,38748E-05 & -0,01758221 & -0,106305883 & 1,45356119 & \dots \\ \vdots & \vdots & \vdots & \vdots & \ddots \end{pmatrix};$$

$$\gamma^{(2)} = \begin{pmatrix} 1,24562E-08 & 2,96456E-06 & 1,59314E-05 & -0,000149424 & \dots \\ 2,96456E-06 & 0,000705566 & 0,003791678 & -0,035562919 & \dots \\ 1,59314E-05 & 0,003791678 & 0,020376288 & -0,191113331 & \dots \\ -0,000149424 & -0,035562919 & -0,191113331 & 1,792490633 & \dots \\ \vdots & \vdots & \vdots & \vdots & \ddots \end{pmatrix};$$

$$\gamma^{(3)} = \begin{pmatrix} 1,6236E-10 & 4,1165E-08 & 9,20847E-07 & 2,14132E-06 & -1,8949E-05 & \dots \\ 4,1165E-08 & 1,0437E-05 & 0,000233473 & 0,000542915 & -0,004804375 & \dots \\ 9,20847E-07 & 0,000233473 & 0,00522272 & 0,012144825 & -0,107472272 & \dots \\ 2,14132E-06 & 0,000542915 & 0,012144825 & 0,028241375 & -0,249914233 & \dots \\ -1,8949E-05 & -0,004804375 & -0,107472272 & -0,249914233 & 2,211546853 & \dots \\ \vdots & \vdots & \vdots & \vdots & \vdots & \ddots \end{pmatrix};$$

$$\gamma^{(4)} = \begin{pmatrix} 5,26177E-10 & 1,32248E-07 & 2,7676E-06 & 4,92362E-06 & -3,85865E-05 & \dots \\ 1,32248E-07 & 3,32391E-05 & 0,000695605 & 0,001237494 & -0,009698272 & \dots \\ 2,7676E-06 & 0,000695605 & 0,014557157 & 0,025897446 & -0,202958992 & \dots \\ 4,92362E-06 & 0,001237494 & 0,025897446 & 0,046072025 & -0,361067725 & \dots \\ -3,85865E-05 & -0,009698272 & -0,202958992 & -0,361067725 & 2,829697678 & \dots \\ \vdots & \vdots & \vdots & \vdots & \vdots & \ddots \end{pmatrix}.$$

We shall notice that the coefficient of masks $\gamma^{(l)}$, $l = \overline{1,4}$ can be determined by taking into account the symmetry of the corresponding matrices.

3. Experimental studies

Operators (6) provide visual enhancement of the perception of digital images distorted by the micro-motion of the fixation chamber, in particular data from the cameras of the target load of aircraft. However, in order to avoid subjectivism in assessing the quality of perception improvement, we present the results of experimental studies that have been conducted using the introduced operators.

Let n, m - raster sizes, $N = n \cdot m$ - the number of pixels of the raster. The image aberration in each pixel is determined as follows:

$$\varepsilon_{i,j} = p_{i,j}^* - p_{i,j}^o, \quad i = \overline{1,n}, \quad j = \overline{1,m},$$

then the average error of reproduction for each component equals

$$\bar{\varepsilon} = \frac{1}{N} \sum_{i=1}^n \sum_{j=1}^m \varepsilon_{i,j};$$

constant error variance –

$$\sigma_{\varepsilon}^2 = \frac{1}{N-1} \sum_{i=1}^n \sum_{j=1}^m (\varepsilon_{i,j} - \bar{\varepsilon})^2.$$

To check the fulfillment of a condition (5) when analyzing reproduced images

widely used is peak-to-peak signal-to-noise ratio - *PSNR*, which is defined as follows:

$$PSNR = 10 \cdot \lg \frac{255^2}{\sigma_{\epsilon}^2} = 10 \cdot \frac{1}{\ln 10} \cdot \ln \frac{255^2}{\sigma_{\epsilon}^2} \cdot$$

The total PSNR for the image is determined by averaging the PSNR of each of the color components. The interpretation of PSNR is quite simple: the greater the value of the statistics is, the greater is the correspondence between the two images.

There has been conducted an experiment for some high-quality digital image. It was aimed at comparison of the performance of the described operators and sharpeners presented in the Adobe PhotoShop CS6 digital image processing environment. In particular, we compared the two filters – “Unsharp Mask” and “Sharpen More filter options” presented in the “Filter” menu and in the “Unsharp Mask” submenu. The use of such filters does not require additional adjustments, so, probably, the filters themselves are operators similar in design (6). Unfortunately, the description of the mentioned filters is not freely available, so the comparative analysis was performed as follows.

Step 1. Generate evenly distributed α , β and require their correspondence with conditions (3) and (4).

Step 2. To test the work of each of the five operators (6) and filters “Unsharp Mask” and “Sharpen More filter options” presented in Adobe PhotoShop CS6, we simulate operator distortion (2) according to the generated α , β and γ mask.

Step 3. Define a PSNR, comparing it to the original image, for each image reproduction result.

Step 4. Repeat the experiment 24 times.

The number of repetitions of the experiment (step 4) is not large, which (unlike the previous experiment) is due to the inability to automate the work with series of images in Adobe PhotoShop CS6. However, as can be seen from the results of the experiment Table 1, even this number of repetitions clearly demonstrates the advantage in the use of filters (6). It is worth paying attention to the following pattern. *PSNR* value according to the results of the use of «Unsharp Mask» filter heavily correlates with *PSNR* values after the use of $C_0(p_{i,j})$ and $C_2(p_{i,j})$ operators, but the filters, researched in this paper, keep the advantage. The same is true for «Sharpen More filter options» filter and operator $C_4(p_{i,j})$.

As it can be seen from the results presented in the table, the introduced operators have advantages in comparison to the well-known «Unsharp Mask» and «Sharpen More filter options».

Table 1. PSNR values after filter comparison experiment with Adobe PhotoShop CS6

№	α	β	γ_0	γ_1	γ_2	γ_3	γ_4	«Unsharp Mask»	«Sharpen More filter options»
1	0,06003	0,00097	39,87	46,42	38,71	32,92	28,77	36,85	28,27
2	0,07743	0,00657	40,36	47,50	39,18	33,24	29,00	37,17	28,43
3	0,08533	0,0009	43,54	51,20	41,88	34,71	30,06	39,73	29,50
4	0,09678	0,01427	40,37	47,68	39,24	33,34	29,08	37,11	28,45
5	0,1226	0,00797	47,77	50,61	45,44	36,49	31,28	42,67	30,58
6	0,1527	0,01274	51,43	46,63	49,14	38,34	32,50	46,10	31,68
7	0,17326	0,02473	50,95	48,90	48,50	37,89	32,17	44,15	31,17
8	0,17365	0,04012	41,40	48,00	40,44	34,45	29,93	37,75	28,99
9	0,22971	0,00407	37,43	36,20	37,76	38,91	36,62	38,42	36,63
10	0,24989	0,00879	36,91	35,77	37,23	38,64	36,98	37,84	37,06
11	0,28518	0,01956	36,47	35,37	36,80	38,60	37,80	37,38	37,92
12	0,29498	0,03736	39,30	37,30	39,92	43,63	39,48	41,13	37,98
13	0,29504	0,03268	38,23	36,59	38,74	41,73	39,36	39,71	38,49
14	0,31059	0,07654	43,04	42,51	43,30	38,79	33,14	40,32	31,24
15	0,36104	0,01354	32,33	32,04	32,44	33,05	33,21	32,44	32,87
16	0,36322	0,02906	33,71	33,15	33,90	35,06	35,95	34,11	35,88
17	0,37001	0,0009	31,11	31,01	31,17	31,44	31,33	31,02	30,49
18	0,37427	0,06638	38,35	36,55	38,97	44,31	42,85	39,87	38,84
19	0,39046	0,08296	39,84	37,71	40,65	46,78	40,30	41,06	35,99
20	0,39988	0,02496	32,03	31,75	32,15	32,77	33,07	32,15	32,77
21	0,4038	0,05305	34,55	33,76	34,82	36,69	38,73	35,21	38,69
22	0,48595	0,10096	35,94	34,75	36,35	39,81	44,01	36,83	38,91
23	0,4881	0,0434	30,89	30,73	30,97	31,40	31,66	30,91	31,19
24	0,49757	0,01782	29,32	29,39	29,35	29,35	29,11	29,08	27,91
Average:			38,55	39,23	38,21	36,76	34,43	37,46	33,33

For a more thorough check of the quality of the restoration we shall introduce the low-frequency noise operators of image distortion and we shall carry out an experiment of simulation modeling according to the following steps.

Step 1. Generate evenly distributed α , β and require their correspondence with conditions (3) and (4).

Step 2. To check how each out of five operators (6) functions we model distortion by the operator (2), according to the generated α , β and γ mask.

Step 3. Define a PSNR, comparing it to the original image, for each image reproduction result.

Step 4. Repeat the experiment 400 times.

The results of the experiment are presented in Table 2. For the sake of clarity, the results of the experiments were sorted by the value of α , and the value of PSNR was averaged within the change intervals of α , (the last column indicates the number of values that were averaged).

Table 2. The value of the averaged PSNR after the experiment was conducted.

α	$\max \beta$	γ_0	γ_1	γ_2	γ_3	γ_4	N
[0,05;0,1)	0.0235	38,73849	44,77572	37,71818	32,35721	28,35858	41
[0,1;0,15)	0.0340	43,98148	49,35406	42,37825	35,04397	30,28478	48
[0,15;0,2)	0.0474	45,7946	46,9347	44,81747	37,56944	32,17712	53
[0,2;0,25)	0.0589	42,83499	41,16095	43,1387	39,88584	34,79463	38
[0,25;0,3)	0.0637	40,7402	38,50291	41,46732	41,71586	36,89772	37
[0,3;0,35)	0.0829	38,37078	36,73771	38,96636	40,56728	37,20889	38
[0,35;0,4)	0.0973	36,43578	35,18418	36,89537	39,81749	37,9436	43
[0,4;0,45)	0.1002	34,04021	33,29069	34,31427	36,23808	36,87641	44
[0,45;0,5)	0.1201	32,73673	32,21276	32,93596	34,41253	35,57243	57
[0,05;0,5]		39,1156	39,7277	38,9605	37,211	37,8732	400

We shall remark, that the maximum PSNR when using the operators (6) is obtained by increasing α ordinary index l . Thus for $C_2(p^{ij})$ maximum PSNR at approximately $\alpha = 0,125$, at the same time for $C_4(p^{ij})$ - at $\alpha = 0,45$ (Fig.1).

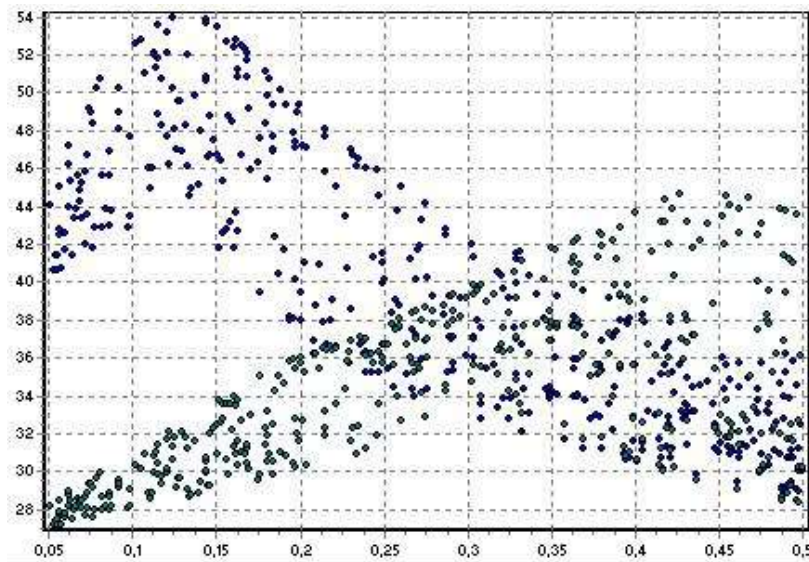


Fig. 1. The values of PSNR when using operators with masks γ_1 (larger values respond for the smaller values of α) and γ_4 : the abscissa axis - α ; the axis of ordinates - PSNR.

Thus, the presented and researched linear operators (6) can be recommended for the automated processing of digital images distorted by interference, such as the micro-movement of the fixation chamber, which is possible for aerial photography from the aircraft.

4. Conclusions

As a result of shooting with digital cameras aimed for different purposes the obtained images can become distorted by the effects of low-frequency hindrance caused by the vibration of the carrier during photo or video shooting. To eliminate the effects of such interference we offer linear filter operators to process the obtained digital images (Fig. 2). In particular, we have presented and experimentally substantiated the linear digital image stabilization operators for the use in case of the random nature of low-frequency interference.

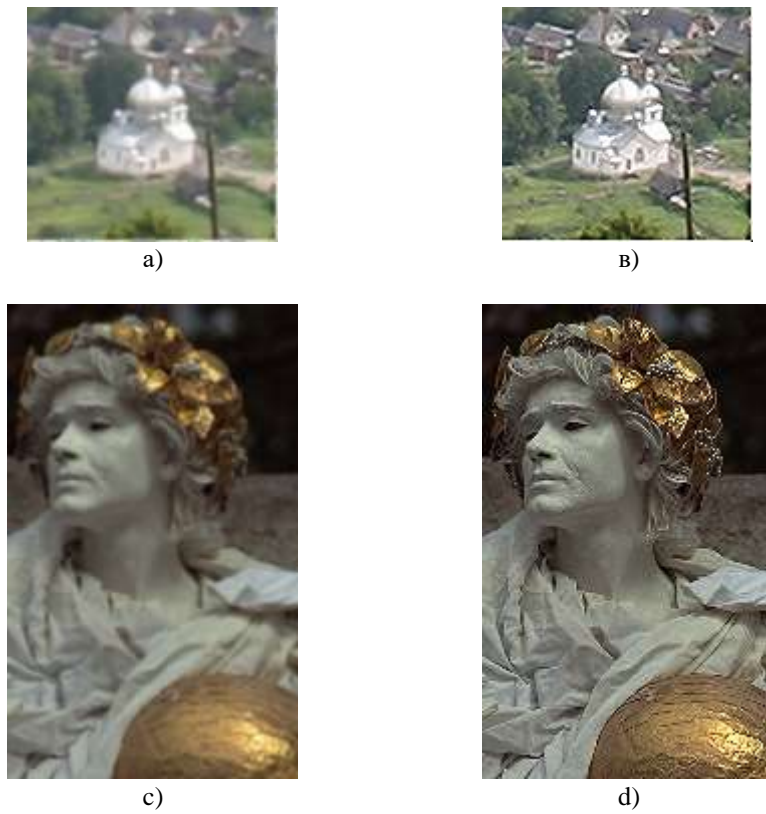


Fig. 2. An example of a digital image: A) and C) – images distorted by a random interference; B) and D) - images after stabilization.

Further research may be aimed at obtaining similar operators with a larger filter mask window width and at the extension of this approach to processing digital video streams in real time for social Internet-services.

References

1. Gruzman I.: Digital image processing in information systems: Textbook / Grusman I., Kyrychuk V., Kosyh V., Peretaygin G., Spector A. – Novosibirsk: Publishig House of the NTU, 2000. – 168 p.
2. The latest image processing techniques. / Ed. A. Potapov. - Moscow: FIZMATLIT, 2008. - 496 p
3. Gonzalez R.: Digital image processing / Gonzalez R., Woods R. - Moscow: Technosphere, 2006. - 1072 p.
4. P. Prystavka "The use of combined filters based on polynomial splines in raster's images processing" // Bulletin of NAU. – 2008. - #4. – P. 104-107.
5. Zohair Al-Ameen, Alaa Muttar, Ghofran Al-Badrani, " Improving the Sharpness of Digital Image Using an Amended Unsharp Mask Filter", International Journal of Image, Graphics and Signal Processing(IJIGSP), Vol.11, No.3, pp. 1-9, 2019.
6. A. Chyrkov "Suspicious Object Search in Video Stream from Aircraft Camera by Using Histogram Analysis", Problems of Creation, Testing and Usage of Information Systems: Scientific Publications of ZhMI, Zhytomyr 13 P. 126-135 (2016).
7. J. Clark, C. Wadhvani, K. Abramovitch, D. Rice and M. Kattadiyil, "Effect of image sharpening on radiographic image quality", The Journal of Prosthetic Dentistry, vol. 120, no. 6, pp. 927-933, 2018.
8. Roman Odarchenko, Serhii Dakov, Olexandr Oksiuk and Larisa Dakova Software-Controlled Network SDN Reliability Calculation 5th International Scientific-Practical Conference Problems of Infocommunications Science and Technology, PIC S and T 2018 - Conference Proceedings, pp 99-103.
9. J. Ye, Z. Shen, P. Behrani, F. Ding and Y. Shi, "Detecting USM image sharpening by using CNN", Signal Processing: Image Communication, vol. 68, pp. 258-264, 2018.
10. F. Ding, G. Zhu, W. Dong and Y. Shi, "An efficient weak sharpening detection method for image forensics", Journal of Visual Communication and Image Representation, vol. 50, pp. 93-99, 2018
11. Prystavka P., Cholyskhina O.: Components of information support for automated processing of digital images based on local operators. Actual problems of automation and information technology: Coll. Sciences. wash. - D .: View of Dnepropetrovsk University – 2010. –T.14. –S.27–36.